

111 211 CR
26186
111

*Annular Suspension and Pointing System
with Controlled DC Electromagnets:
ECE 485 Senior Design Project Report*

N95-12666

Unclas

G3/37 0026186

by

Josephine Lynn, Vu, and Kwok Hung, Tam,
Student, Old Dominion University.

Submitted to

Dr. Vahala and Dr. Britcher,
Instructors, Old Dominion University.

April 22, 1993

(NASA-CR-197206) ANNULAR
SUSPENSION AND POINTING SYSTEM WITH
CONTROLLED DC ELECTROMAGNETS (Old
Dominion Univ.) 51 p

Pledge:

Tam, Kwok Hung

Josephine L. Vu

<u>Table of contents</u>	Page
I. Introduction	6
A. Problem definition	6
B. Project Objectives	10
C. Summary	10
II. Modelling of single degree ASPS bearing actuator	11
A. Assumptions of the model	11
B. Derivation of ASPS dynamics	12
a. B-field in the gap	12
b. Relationship between F, I and g	14
c. V-I relationships of the actuator	16
d. Discussion of the plant dynamic of ASPS actuator	20
III. Compensator design	22
A. Cascade compensator	22
B. Feedback compensator	27
IV. Computer simulation	32
V. Discussion of results	36
VI. Conclusion and recommendation	38
Bibliography	39
Appendix I: root locus results of the general lead lag cascade compensator	41
Appendix II: root locus results of the cascade dual phase advance compensator	42
Appendix III: state feedback design procedure	44
Appendix IV: computer codes for nonlinear plant dynamics	48

Illustrations

	Page
Figure 1. ASPS outlook	7
Figure 2. ASPS actuators arrangement	8
figure 3. coupling and decoupling matrixes	9
Figure 4. configuration of actuator	11
Figure 5. pole zero diagram of open loop plant	22
Figure 6. root locus of open loop plant	24
Figure 7. block diagram of cascade compensator	25
Figure 8. step response--cascade compensator	26
figure 9. Bode plot--cascade compensator	27
Figure 10. state space diagram of open loop plant	28
Figure 11. block diagram of feedback compensator	30
Figure 12. step response--feedback compensator	31
Figure 13. Bode plot--feedback compensator	32
Figure 14. step response with linear equation	35
Figure 15. step response, velocity, linear	36
Figure 16. step response, acceleration, linear	36
Figure 17. step response, position, nonlinear	36
Figure 18. step response, velocity, nonlinear	36
Figure 19. step response, current, nonlinear	36
Figure 20. state diagram of estimator and controller	48

List of Symbols

A: cross-sectional area of one side of the actuator
a: assigned constant
B: magnetic flux density in the gap
B_m: magnetic flux density inside the actuator
b: assigned constant
c²: assigned constant
F(x,i): attractive force between the actuator and the rim(suspended mass)
G_p(s): plant dynamic equation or open loop transfer function
g₁, g₂, g: gap distance
g_o: equilibrium distance
I: input current of the actuator
I_b, I_o: equivalent bias current
i: controlled current
L: inductance of the actuator
L_c: inductance of the coil
L₁: inductance of the gap
l: the length of actuator
m: mass of the rim(suspended mass)
N: number of turns of the coil
R: actuator resistance
s: Laplace transform variable
V: input voltage of the actuator
V_b: equivalent bias voltage
v: controlled voltage
x: controlled distance or small perturbation distance from

equilibrium

μ : permeability of the actuator material

μ_c : permeability of free space

ϕ : magnetic flux

L.H.P : left half plane

ASPS : Annular Suspension and Pointing System

I. Introduction

A. Problem Definition

Frictionless electromagnetic suspension and levitation has attracted much attention since 1970. Applications include high-speed machine tool spindles, ultra-centrifuges, high vacuum pumps, and fly-wheels for energy storage. Methods of producing

electromagnetic suspension and levitation include controlled DC electromagnets, diamagnetic materials, superconductors, hybrid systems, and tuned LCR circuits. A comprehensive review lecture of electromagnetic suspension and levitation techniques can be found in reference 1.

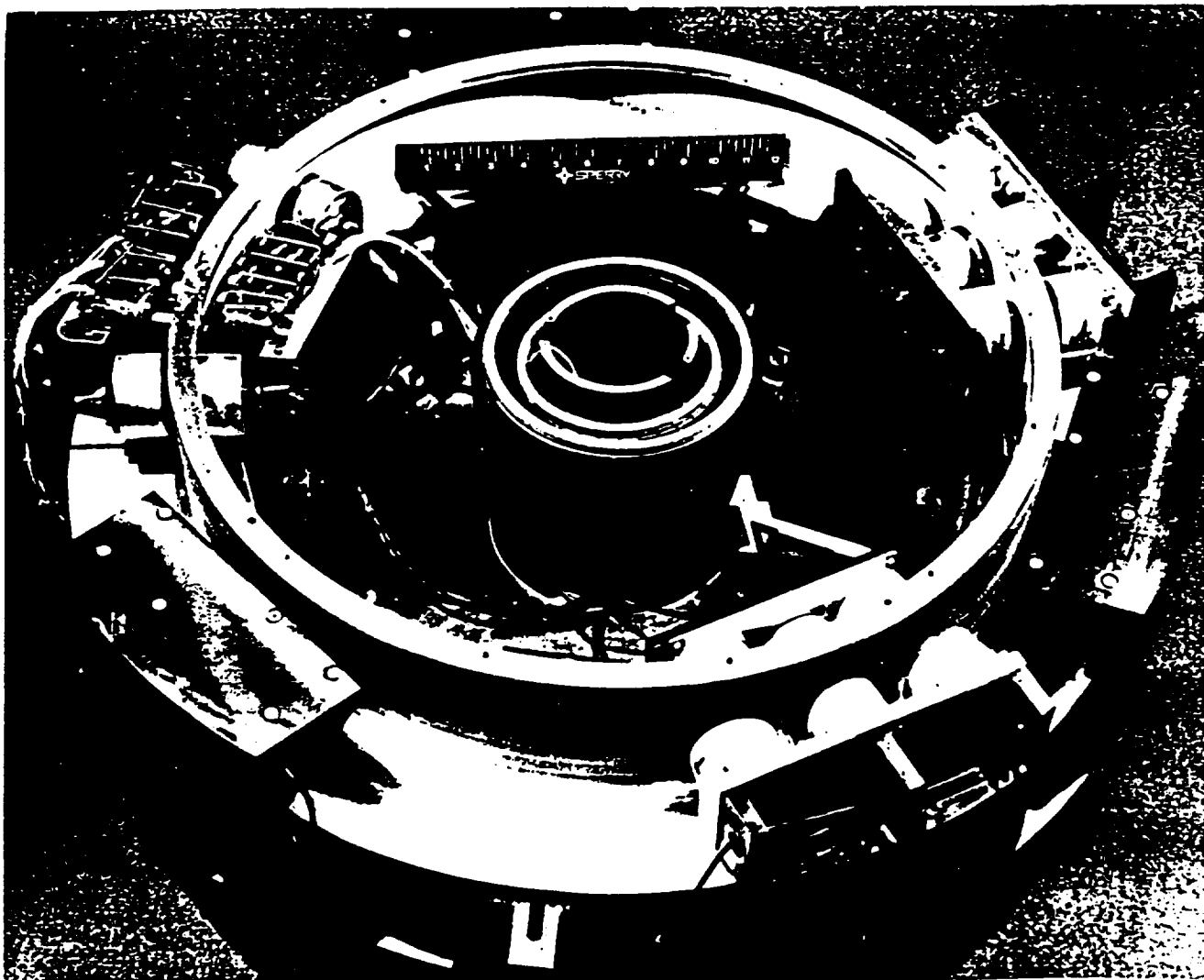
The technique of suspension and levitation with controlled DC electromagnets is the most advanced and successful at this time. Many investigations are underway worldwide. Advanced ground transportation schemes, contactless bearings for ultra-high speed, and gyroscopes have been successfully demonstrated by many groups of researchers.¹

The Annular Suspension and Pointing System (ASPS) developed by the Flight System division of Sperry Corporation¹ is a six-degree of freedom payload pointing system designed for use with the space shuttle. This magnetic suspension and pointing system provides precise controlled pointing in six-degrees of freedom, isolation of payload-carrier disturbances, and end mount controlled pointing. Those are great advantages over the traditional mechanical joints for space applications. More detail discussions of the magnetic suspension joints and mechanical joints can be found in reference

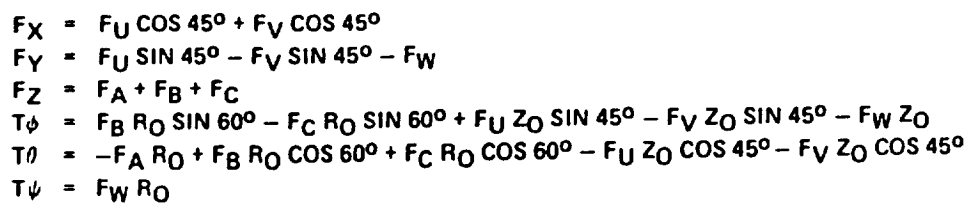
2.

Figure 1 and 2 show the ASPS designed by Sperry Corporation. It consists of six actuators, three for vertical movements, two for radial movements, and one for tangential movements. By the coupling and decoupling matrices (figure 3) ², we can carefully decompose the command signal of each degree of freedom to each actuator individually. In other words, the coupling and decoupling matrices change the six-degree of freedom ASPS control system to six single-degree of freedom ALPS control systems. Hence, we can design each control loop separately.

figure 1.



VERNIER ACTUATOR FORCES AND MOMENTS



VERNIER ACTUATOR DECOUPLING

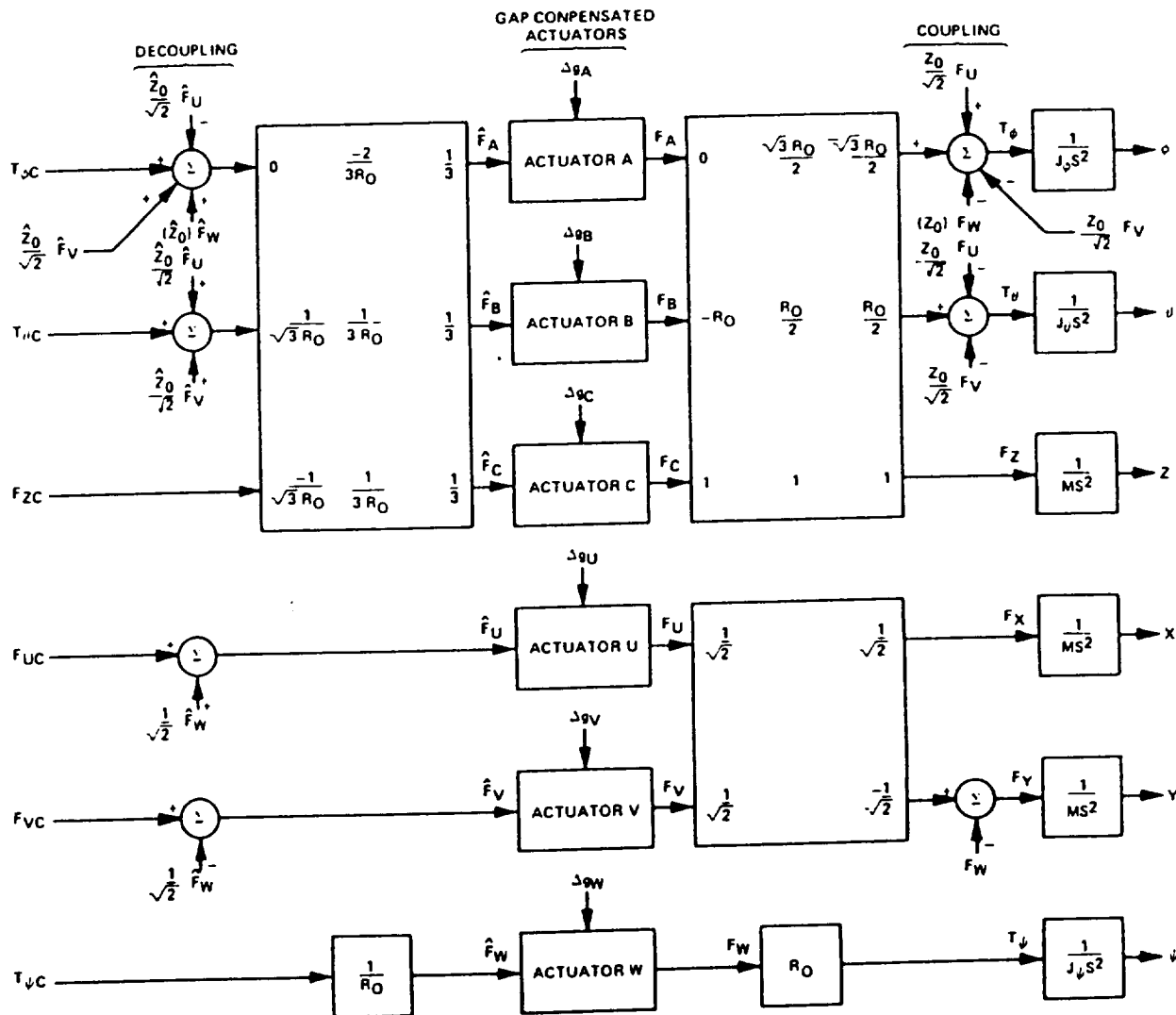


FIGURE 3

B. Project Objectives

- (i) Understanding the existing ASPS in the lab.
- (ii) Model the dynamics of a single DC controlled ALPS actuator as accurately as possible.
- (iii) Re-design a controller for the single degree of freedom ALPS control system to achieve the highest stiffness as possible. {Highest stiffness will have the lowest motion in response to external forces}

C. Summary

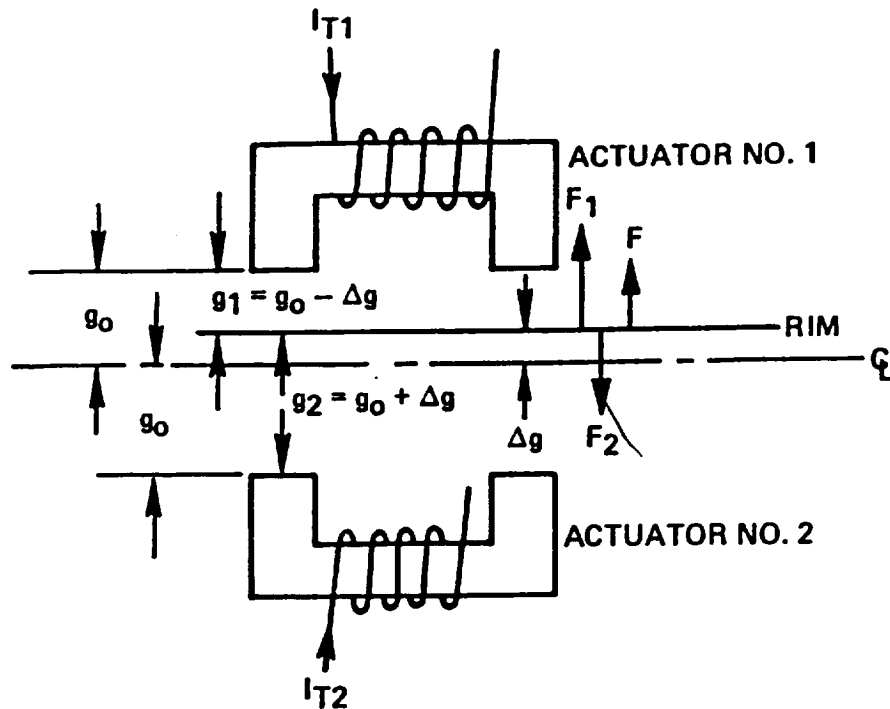
In this design, we first analyzed the assumed model of the single degree ASPS bearing actuator, and obtained the plant dynamics equations. By linearizing the plant dynamics equations, we designed the cascade and feedback compensators such that a stable and satisfied result was obtained. The specified feedback compensator was computer simulated with the nonlinearized plant dynamics equations. The results indicated that an unstable output occurred. In other words, the designed feedback compensator is fail. The failure of the design is due to the Taylor's series expansion does not converge.

II. Modelling of the single degree ASPS bearing actuator

A. Assumptions of the model

The single degree ASPS bearing actuator consists of two pairs of magnetic coil elements, mounted in opposition, to control the rim (suspended mass) along a single axis. Figure 4 shows the configuration of the actuator. The magnetic coil elements have current biasing superimposed by a controlled DC voltage source to produce a force to suspend and point the rim. For fine pointing application, the gap distances between the rim and actuators are kept to a predetermined value ($<0.3''$).

figure 4.



We derived the equation for the single ALPS bearing actuator with the following assumptions:

(i) The force of attraction between magnetized bodies is given by $F = (1/2\mu) * B^2 * \text{area}$.

(ii) The magnetic flux density is uniform between the gap, or gap distance \ll size of actuator.

(iii) The rim is a perfect conductor. That is, it does not support any magnetic field strength (H) inside the rim.

(iv) There is no coupling effect between each coil elements.

(v) The controlled electromagnet behaves linearly, and there is no loss or fringing of magnetic field.

(vi) The rim has a plane area over the magnetic coil assemblies.

B. Derivation of ASPS Dynamics

a) B-field in the air-gap.

From magnetic circuit theory, the total current linked by the path of an N-turn coil is given by

$$\sum_i H_i l_i = N i \quad (4)$$

Assume

(i) the magnetic material is approximated by $B_m = \mu_m H_m + B_0$ where B_0 is a constant.

(ii) gap distant at path (1) = gap distance at path (2)

ie. $g_1 = g_2 = g$

(iii) from boundary condition, B inside the coil \approx B in

the gap.

Therefore, equation (1) becomes,

$$\begin{aligned}
 H_1 g_1 + H_2 g_2 + H_m l &= Ni \\
 \rightarrow 2Hg + \frac{B_m - B_o}{\mu_m} l &= Ni \quad \text{(because the rim is a perfect conductor)} \\
 \rightarrow 2Hg + \frac{\mu_o}{\mu_m} l H &= Ni + \frac{B_o l}{\mu_m}
 \end{aligned}$$

As the term $B_o(l/\mu_m)$ can be equivalently assigned to a magnetomotive force (mmf) $(B_o/\mu_m)l = NI_o$.

So

$$2Hg + \frac{\mu_o l}{\mu_m} H = Ni + NI_o$$

Thus the magnetic flux density at the gap is given by

$$B = \mu_o H = \frac{\mu_N (i + I_o)}{2g + \frac{\mu_o l}{\mu_m}}$$

As for the particular material we used for actuator, $\mu_m \gg \mu_o$.

Hence

$$B = \frac{\mu_o N (i + I_o)}{2g} \quad (2)$$

b) Relationship between F, I and g

By considering the stored magnetic energy, Bohr⁵ and Hayt⁶ were able to relate the magnetic attraction force to the magnetic flux density and cross-sectional,

$$F_m = \frac{1}{2\mu_o} B^2 * area$$

The geometry we used is similar to Humphris⁷ and Groom⁸, figure 4, which have two electromagnets positioned opposite the rim. This kind of configuration is more linear if we separate the magnetic flux density into the controlled and bias components.⁷

Assume no coupling effect between the two actuators, by equation (2):

$$B_1 = \frac{\mu_o N_1 (i_1 + I_1)}{2g_1}; B_2 = \frac{\mu_o N_2 (i_2 + I_2)}{2g_2}$$

Let $N_1 = N_2 = N$, $I_1 = I_2 = I_o$, $i_1 = -i_2 = i$ = controlled current. Therefore, the total force acting on the rim is given by

$$F = F_1 - F_2 = \frac{(2A)}{2\mu_o} (B_1^2 - B_2^2) = \frac{A}{\mu_o} (B_1 + B_2) (B_1 - B_2)$$

$$\text{Consider } B_1 - B_2 = \frac{\mu_o N}{2} \left[\frac{I_o + i}{g_o - x} - \frac{I_o - i}{g_o + x} \right]$$

$$= \frac{\mu_o N}{2} \left[\frac{(g_o + x)(I_o + i) - (g_o - x)(I_o - i)}{g_o^2 - x^2} \right]$$

$$= \frac{\mu_o N}{2(g_o^2 - x^2)} [g_o(I_o + i - I_o + i) + x(I_o + i + I_o - i)]$$

$$= \frac{\mu_o N}{2(g_o^2 - x^2)} (2g_o i + 2I_o x) = \frac{\mu_o N(g_o i + I_o x)}{g_o^2 - x^2}$$

$$\text{Similiarly, } B_1 + B_2 = \frac{\mu_o N}{2} \left[\frac{I_o + i}{g_o - x} + \frac{I_o - i}{g_o + x} \right] = \frac{\mu_o N}{g_o^2 - x^2} (g_o I_o + xi)$$

$$\begin{aligned} \text{Thus } F &= \frac{A}{\mu_o} (B_1 + B_2) (B_1 - B_2) = \frac{A}{\mu_o} \left[\frac{\mu_o N(g_o i + I_o x)}{g_o^2 - x^2} \right] \left[\frac{\mu_o N(g_o I_o + xi)}{g_o^2 - x^2} \right] \\ &= \frac{\mu_o N^2 A (g_o i + I_o x) (g_o I_o + xi)}{(g_o^2 - x^2)^2} \end{aligned}$$

By the Taylor's Series Expansion at the equilibrium point (x_o, i_o) , we get

$$F(x, i) = F(x_o, i_o) + (x - x_o, i - i_o) * \nabla F|_{(x_o, i_o)}$$

$$\text{as } \frac{\partial F}{\partial i} = \frac{\mu_o N^2 A}{(g_o^2 - x^2)^2} [g_o(g_o I_o + xi) + x(g_o i + I_o x)]$$

$$\begin{aligned} \frac{\partial F}{\partial x} &= \frac{\mu_o N^2 A}{(g_o^2 - x^2)^4} [(g_o^2 - x^2)^2 [I_o(g_o I_o + xi) + i(g_o i + I_o x)] \\ &\quad - 2(g_o^2 - x^2)(-2x)(g_o I_o + xi)(g_o i + I_o x)] \end{aligned}$$

at equilibrium point $(x_o, i_o) = (0, 0)$,

$$F(x_o, i_o) = 0$$

$$\frac{\partial F}{\partial x}|_{(x_o, i_o)} = \frac{\mu_o N^2 A I_o^2}{g_o^3}$$

$$\frac{\partial F}{\partial i}|_{(x_o, i_o)} = \frac{\mu_o N^2 A I_o}{g_o^2}$$

So

$$\begin{aligned} F(x, i) &= x * \frac{\partial F}{\partial x}|_{(x_o, i_o)} + i * \frac{\partial F}{\partial i}|_{(x_o, i_o)} \\ &= \left(\frac{\mu_o N^2 A I_o^2}{g_o^3} \right) x + \left(\frac{\mu_o N^2 A I_o}{g_o^2} \right) i \end{aligned} \tag{3}$$

c) V-I relationship of the actuator.

Recall equation (2):

$$B = \frac{\mu_o N(i + I_o)}{2g}$$

By definition, $\Phi = NBA$ and $L = (d\Phi/di)^5$. Therefore, the inductance of the gap is

$$L_1 = NA \frac{dB}{di} = \frac{N^2 A \mu_o}{2g} \quad (4)$$

and the inductance of the whole circuit is

$$\begin{aligned} L &= L_1 + L_2 + L_c = \\ &= \frac{N^2 A \mu_o}{2g_1} + \frac{N^2 A \mu_o}{2g_2} + L_c \\ &= \frac{N^2 A \mu_o g_o}{g_o^2 - x^2} + L_c \end{aligned} \quad (\text{by 4})$$

By Kirchhoff's voltage law, we have

$$\begin{aligned} V &= Ri + \frac{d}{dt}(Li) \\ &= Ri + L \frac{di}{dt} + i \frac{dL}{dx} * \frac{dx}{dt} \end{aligned}$$

We previously separated the voltage, current and gap distance into the bias components and controlled components.

$$\text{That is Let } V = V_b + v$$

$$i = I_b + i$$

$$\text{and } x = g_o + x$$

Therefore,

$$V_b + v = R(I_b + i) + L \frac{di}{dt} + i \frac{dL}{dx} * \frac{dx}{dt} + I_b \frac{dL}{dx} * \frac{dx}{dt}$$

As, at equilibrium position, $V_b = RI_b$, assume $i \approx 0$, $x \approx 0$

Therefore,

$$i \frac{dL}{dx} * \frac{dx}{dt} \approx 0$$

$$\text{so } v = Ri + L \frac{di}{dt} + I_b \frac{dL}{dx} * \frac{dx}{dt}$$

$$\text{Consider } \frac{dL}{dx} = \frac{2N^2 A \mu_o g_o}{g_o^2 - x^2} x$$

$$\therefore I_b * \frac{dL}{dx} * \frac{dx}{dt} = I_b \frac{2N^2 A \mu_o g_o}{(g_o^2 - x^2)^2} * x * \frac{dx}{dt} \approx 0$$

$$\text{Thus } v(t) = Ri(t) + L \frac{d}{dt} i(t)$$

taking the Laplace transform on both sides, we get

$$V(s) = RI(s) + LsI(s)$$

$$\text{or } I(s) = \frac{1}{R + Ls} V(s) \quad (5)$$

Recall equation (3)

$$F(x, i) = \frac{A\mu_o N^2 I_o^2}{g_o^3} x + \frac{A\mu_o N^2 I_o}{g_o^2} i$$

By Newton Second Law $F(x, i) = m \frac{d^2 x}{dt^2}$

$$\text{So, } m \frac{d^2 x}{dt^2} = \frac{A\mu_o N^2 I_o^2}{g_o^3} x + \frac{A\mu_o N^2 I_o}{g_o^2} i$$

Taking the Laplace Transform on both sides, we get

$$ms^2 X(s) = \frac{A\mu_o N^2 I_o^2}{g_o^3} X(s) + \frac{A\mu_o N^2 I_o}{g_o^2} * \frac{1}{R + Ls} V(s)$$

$$\text{or } \frac{X(s)}{V(s)} = \frac{\frac{A\mu_o N^2 I_o}{g_o^2}}{(R + Ls) (ms^2 - \frac{A\mu_o N^2 I_o^2}{g_o^3})} \quad (6)$$

$$= \frac{\frac{A\mu_o N^2 I_o}{g_o^2 mL}}{(s + \frac{R}{L}) (s^2 - \frac{A\mu_o N^2 I_o^2}{m g_o^3})}$$

$$\text{Let } a = \frac{A\mu_o N^2 I_o}{g_o^2 mL}, \quad b = \frac{R}{L}, \quad c^2 = \frac{A\mu_o N^2 I_o^2}{m g_o^3}$$

Therefore the plant dynamics of the ALPS actuator are

$$G_p(s) \triangleq \frac{X(s)}{V(s)} = \frac{a}{(s + b) (s^2 - c^2)}$$

Which is similar to the plant dynamic equation obtained by

Kilgore⁹ and Jayawant³.

Referring to Groom², the values of those parameters are,

I_0	0.57 Amps
A	$1.1400918 \times 10^{-3} \text{ m}^2$
μ_0	$4 \pi \times 10^{-7} \text{ H m}^{-1}$
N	1386 turns per coil
m	7.19712 kg
g_0	0.00762 m
R	8.0 Ω
L	0.1805899 h at g_0

$$\therefore a \approx 20.79$$

$$b = 44.3$$

$$c^2 \approx 280.8$$

Thus, the open loop transfer function is

$$G_p = \frac{20.79}{s^3 + 44.3s^2 - 280.8s - 12439.59}$$

d) Discussion of the plant dynamic of ASPS actuator

The open loop transfer function is a third order, type zero, all poles plant system. The characteristic equation also contains one positive real root, so this plant is not BIBO stable. The pole zero diagram of the plant is shown in fig 5. In order to move the open loop unstable root into the stable region, we need to add zeros in the left half plane so that the locus are pulled into the stable region. In other word, a reshaping of the root locus (compensator) is necessary.

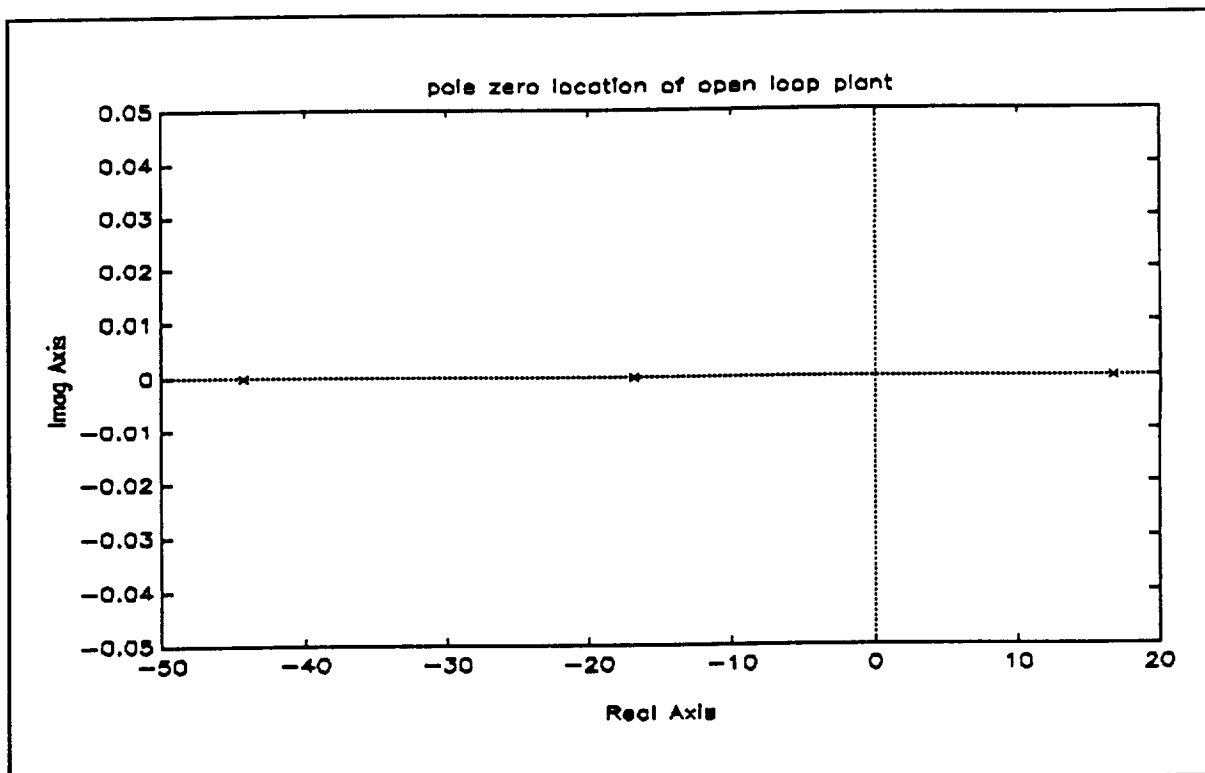


figure 5

III. Compensators Design

A. Cascade Compensator

The approach we used in the cascade compensator is to achieve the goal (shift the root locus to the L.H.P.) with minimum complexity. For the simplest case, by the knowledge that a pole will pull the root locus to the right, a zero will pull the root locus to the left and a pole-zero pair close to the origin will decrease the steady state step error (G_p is type zero), we tried the general lag-lead cascade compensator¹⁰,

$$G_c(s) = A \frac{(s + \frac{1}{T_1})}{(s + \frac{1}{\alpha T_1})} \frac{(s + \frac{1}{T_2})}{(s + \frac{\alpha}{T_2})}$$

with $\alpha = 10$, and gain A. ¹⁰ The lag component was fixed at

$(s + 0.05)/(s + 0.005)$ and the lead component was moved along the real axis. Some root locus results are shown in appendix I. After studying the results, we decided that we needed to increase the compensator complexity in order to meet the design specifications.

Since the lag component only affected the steady state error, for simplicity, we tried the dual phase advanced compensator with $\alpha = 10$.

$$G_c(s) = \left(\frac{s + \frac{1}{T}}{s + \frac{\alpha}{T}} \right)^2$$

Some root locus results were shown in the appendix II.

Interestingly, when we put the double zero near to the second large negative real pole of the open-loop transfer function, a significant portion of the root locus were pulled into the left half plane, figure 6. This was the result we were looking for.

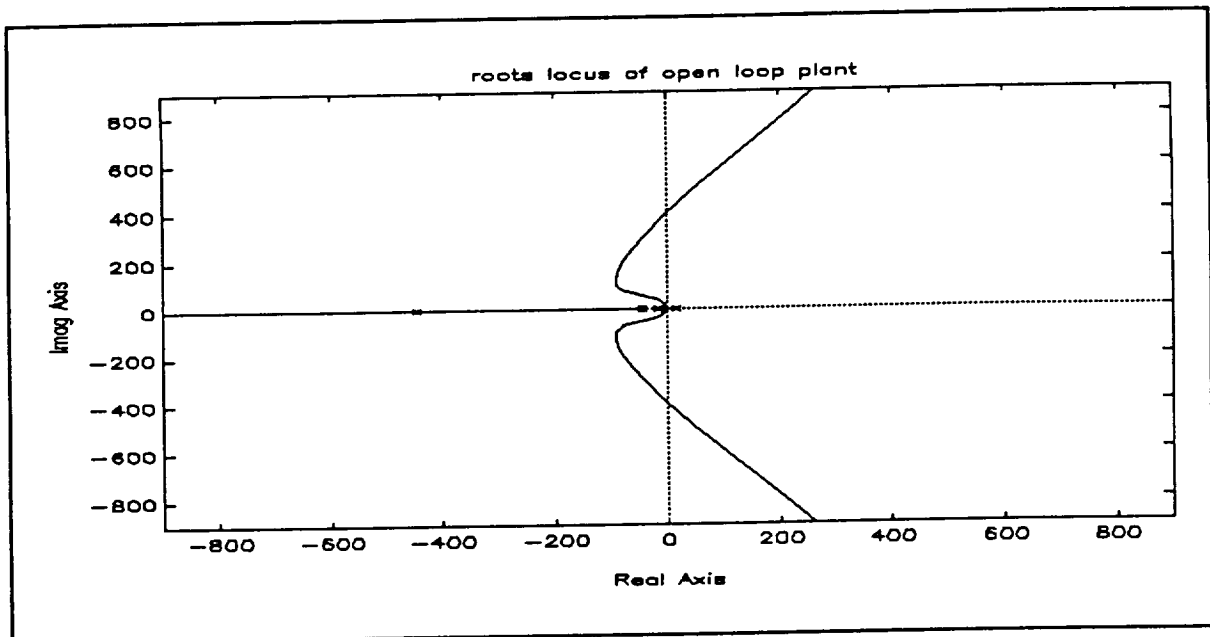


figure 6

Addition of a lag component in the compensator only reduced the steady state step error slightly (0.02), so for simplicity, we used the dual phase advanced compensator

$$G_c(s) = \left(\frac{s + 44.3}{s + 443} \right)^2$$

A block diagram is shown in figure 7. We selected a damping ratio $\xi = 0.7$, and the maximum natural frequency. The figures of merit are,

poles: $-86.15 \pm 87.89j$, -93.24 , -620.46

additional gain $K = 1.011406 \text{ E } 6$

steady state step error = 0.06

rise time = 0.009 sec.

peak overshoot = 1.42

peak time = 0.025 sec.

settling time = 0.05 sec. (for 5%)

gain margin = 16.75 dB

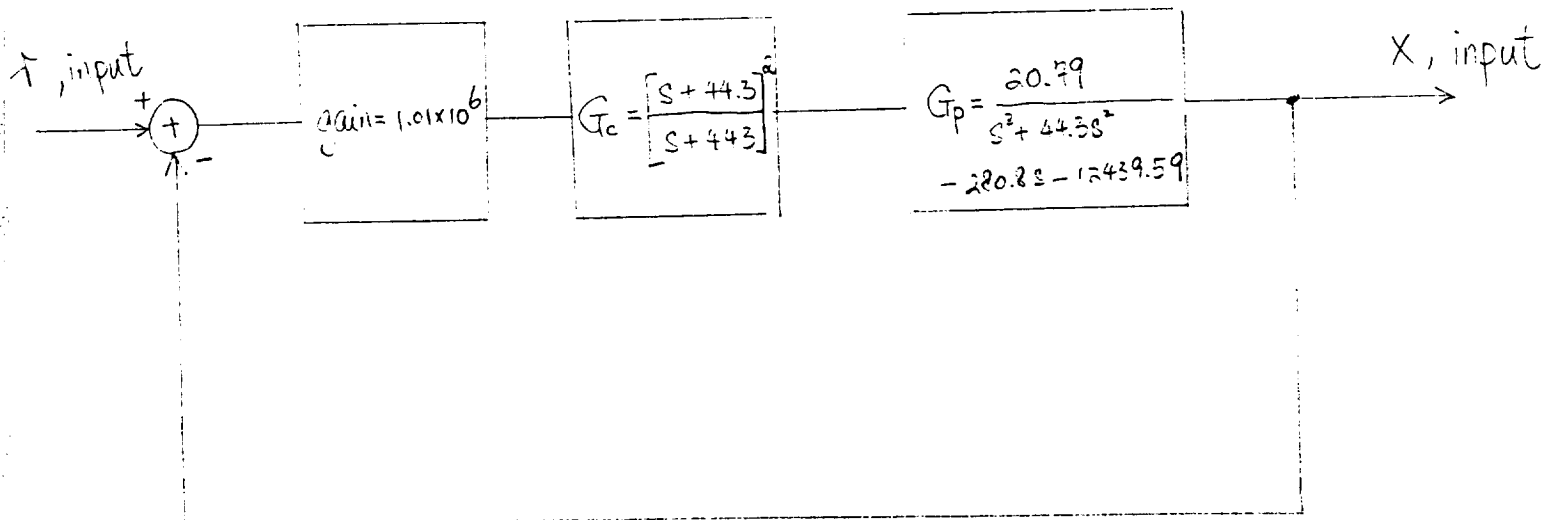
phase margin = 180°

stiffness, $\omega_n = 15 \text{ kN kg}^{-1}\text{m}^{-1}$

stability region : $6.0939 \text{ E } 4 < K < 6.8041 \text{ E } 6$

The step response was shown in figure 8, and the Bode plot was shown in figure 9. Those results are obtained by matlab.

figure 7.



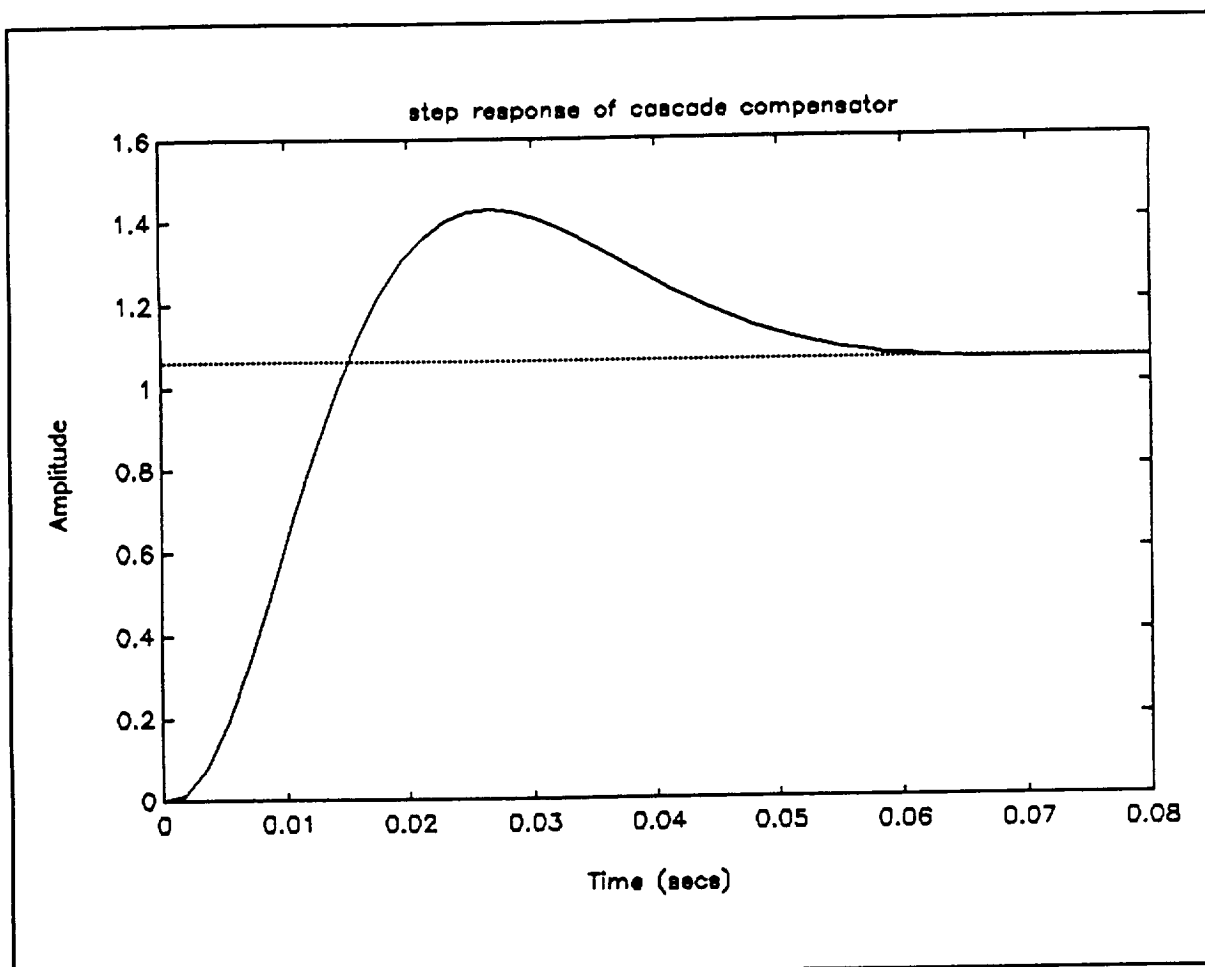


figure 8

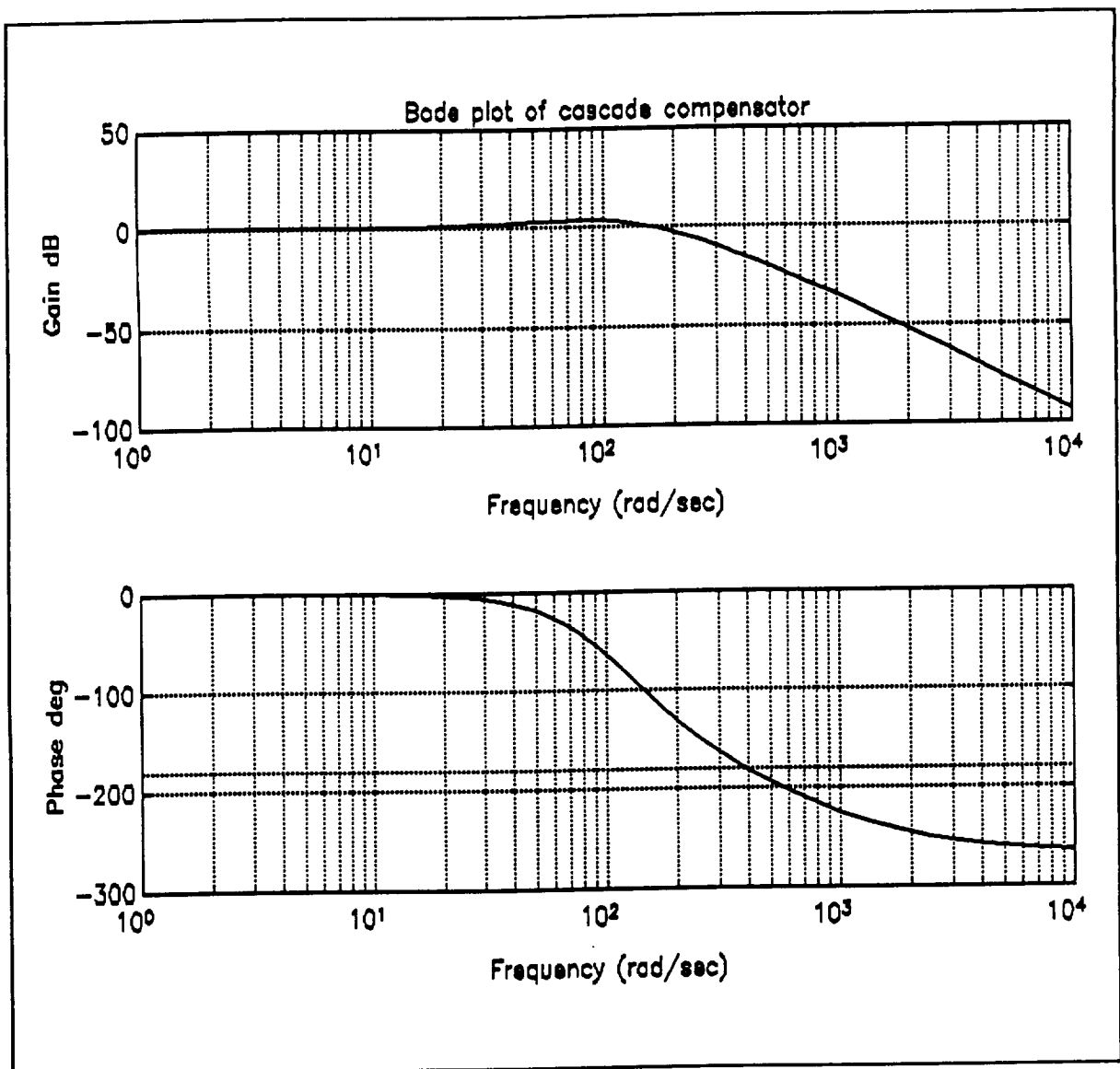


figure 9

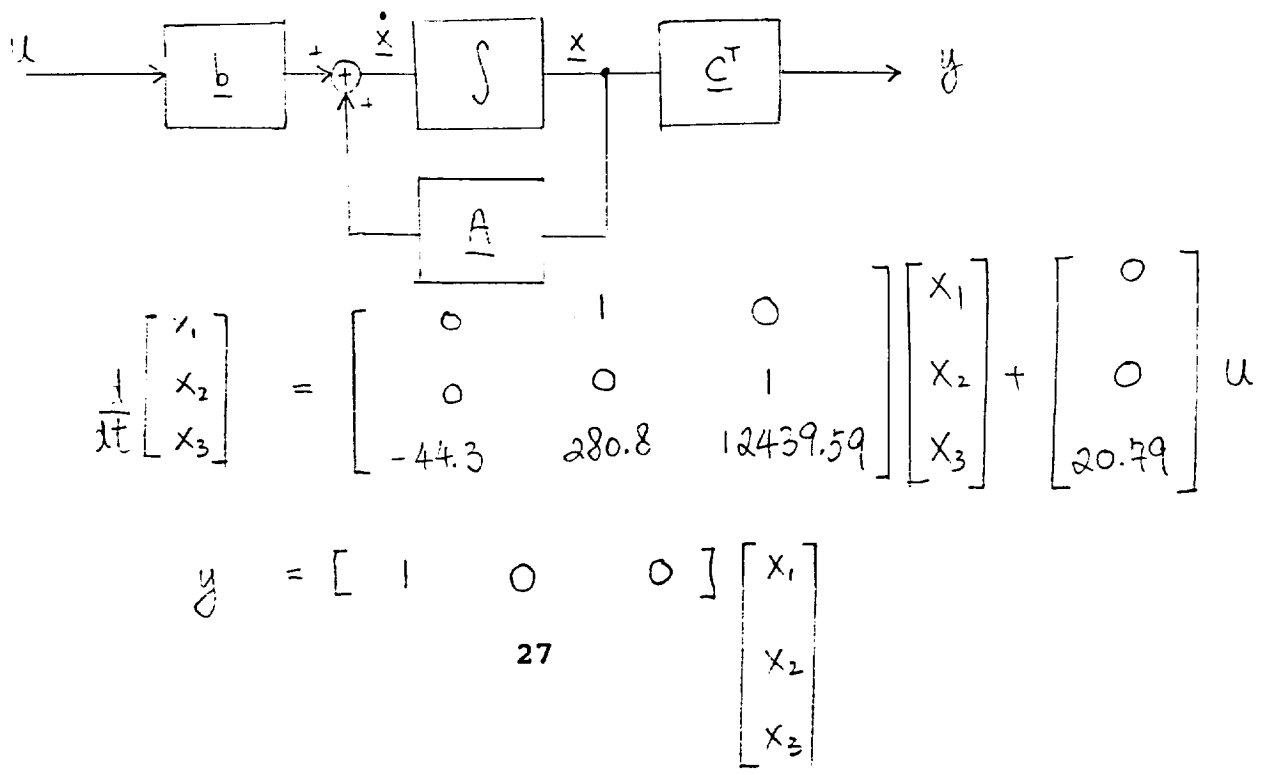
B. Feedback Compensator Design

The cascade compensator will be converted to a digital controller later, and a computer will be involved to control the plant. Therefore, it is natural to design the compensator using the state feedback technique. This technique is flexible and convenient to implement. A brief derivation of the design procedure is shown in Appendix III. In the case where some state variables are not accessible, an observer (estimator) may be used. Observer design procedures are also shown in the Appendix III. This material are come D'Azzo ¹⁰. In this design, we used the full state feedback technique.

A state space representation of the open loop plant is shown in the figure 10.

figure 10

State space representation of the open loop plant



The controllability matrix is,

$$M_c = [b | Ab | A^2b]$$

=

$$\begin{vmatrix} 0 & 0 & 20.79 \\ 0 & 20.79 & -920.997 \\ 20.79 & -920.997 & 46637.99 \end{vmatrix}$$

as $\det(M_c) \neq 0$, so M_c has full rank.

The observability matrix is

$$M_o = [C^T | A^T C^T | (A^T)^2 C^T]$$

=

$$\begin{vmatrix} 1 & 0 & 0 \\ 0 & 1 & 0 \\ 0 & 0 & 1 \end{vmatrix}$$

So M_o has full rank. Hence, this system is completely controllable and completely observable.

Motivated by the performance of the cascade compensator, we selected the poles of the control ratio to be $-86.15 \pm 87.89j$, -100 , which give us a good step response. A block diagram is shown in the figure 11. The figures of merit are,

$$\text{gain} = 72.8546 \text{ E } 3$$

$$k_1 = 1.01$$

$$k_2 = 0.021561$$

$$k_3 = 0.0001505$$

$$\text{poles : } -86.15 \pm 87.89j, -100$$

$$\text{steady state step error} = 0$$

$$\text{rise time} = 0.03 \text{ sec.}$$

$$\text{settling time} = 0.045 \text{ sec. (for 5 \%)}$$

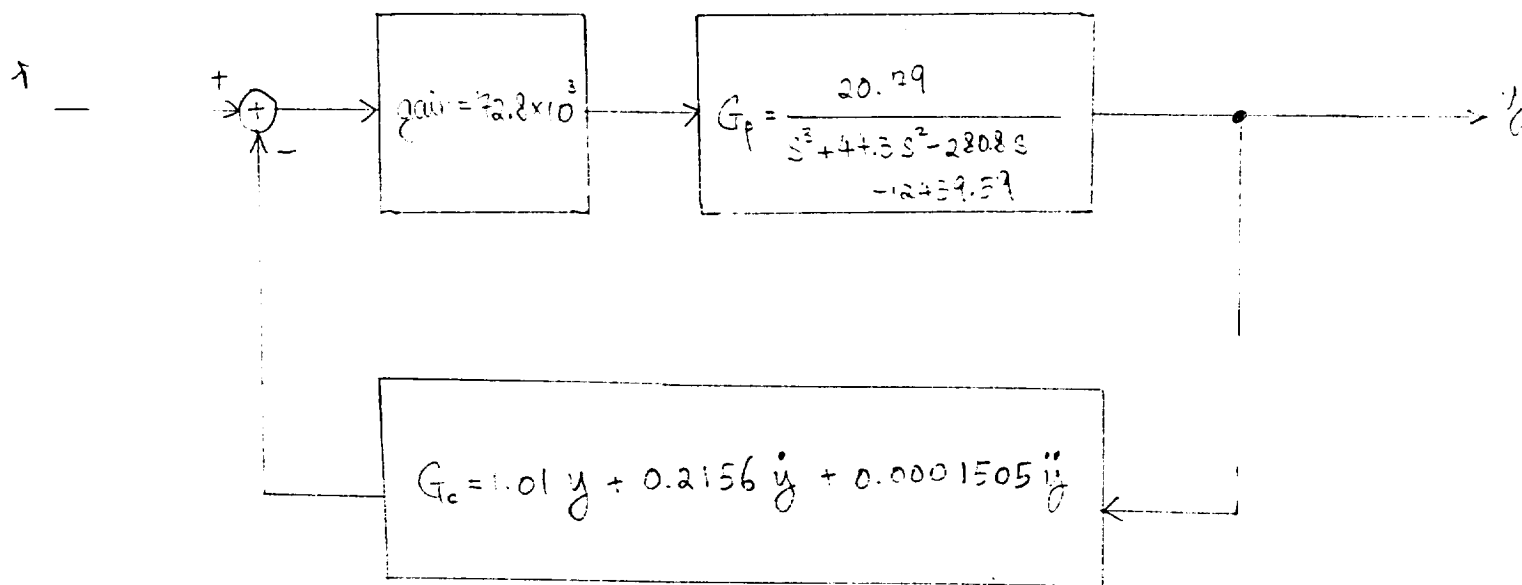
$$\text{gain margin} = 13 \text{ dB}$$

$$\text{phase margin} = 160^\circ$$

$$\text{stiffness} = 15 \text{ kNkg}^{-1} \text{ m}^{-1}$$

A step response and Bode plot were shown in figure 12 and figure 13 respectively. Those results are obtained by matlab.

figure 11.



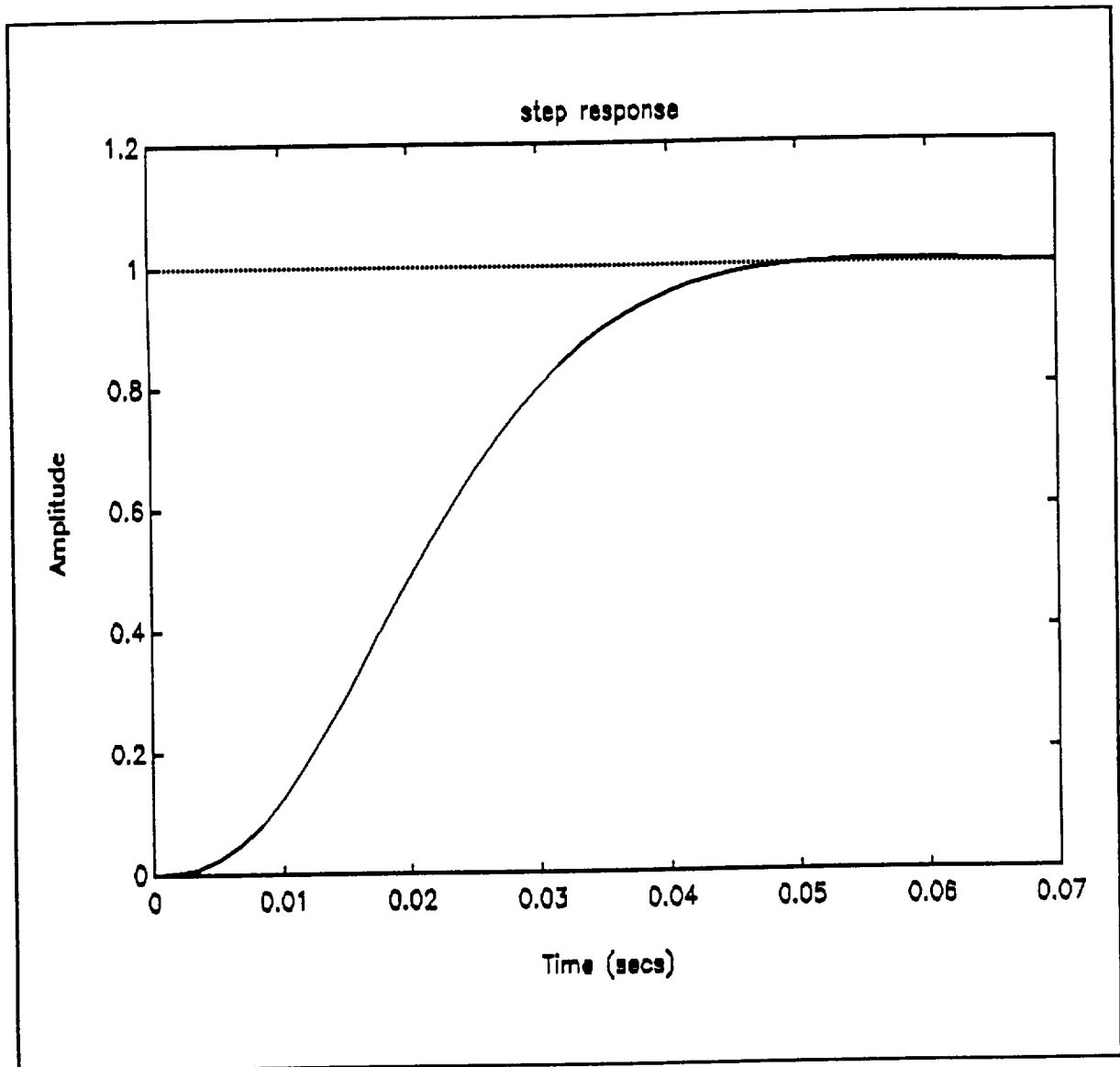


figure 12

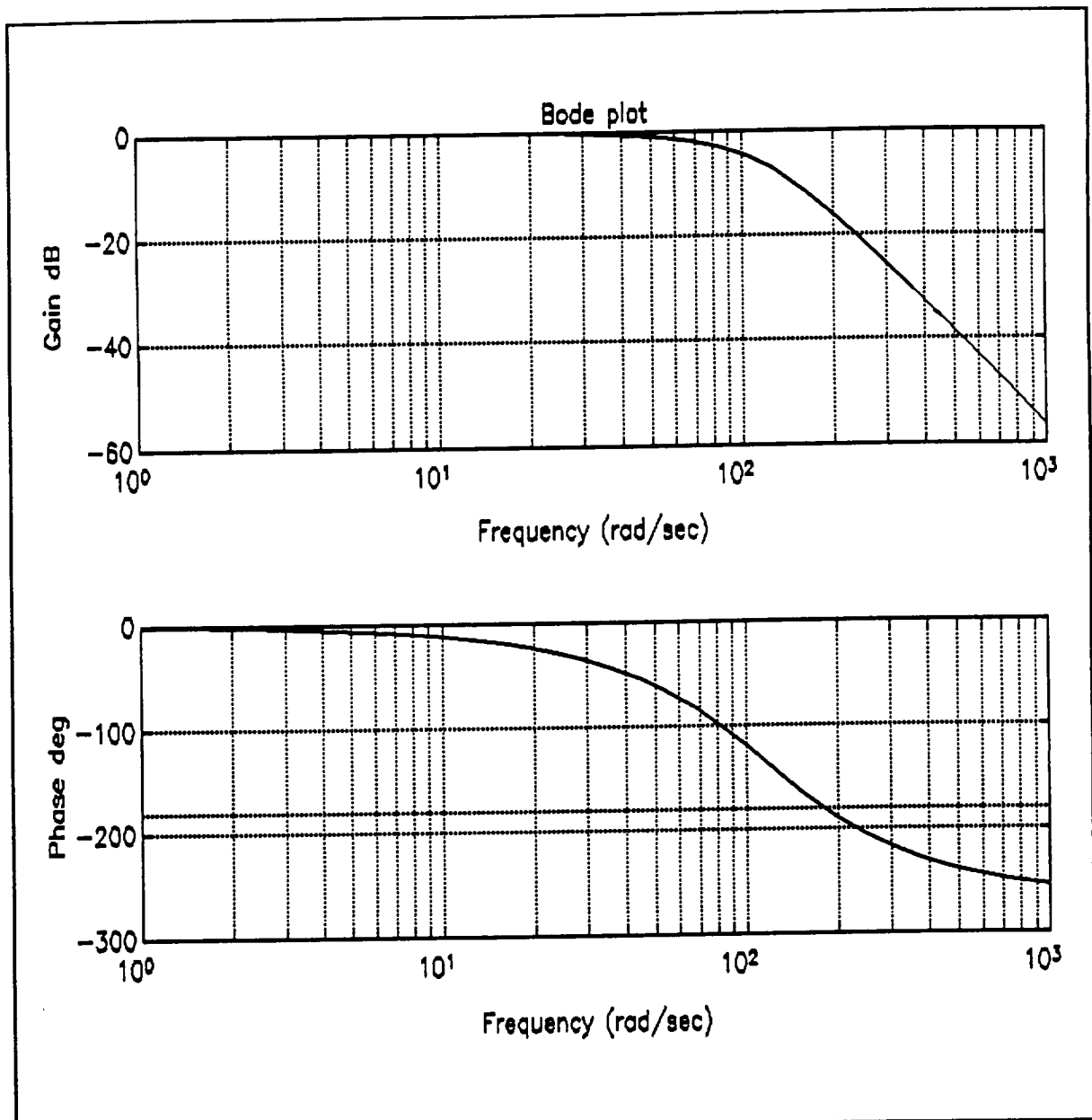


figure 13

IV Computer Simulation

We simulated the state feedback design by a four order Runge Kntta Method in the time domain. The Runge Kntta Method is a special version of the general Taylor's series expansion.

For a general different equation,

$$\frac{d\vec{X}}{dt} = \vec{f}(\vec{X})$$

Let,

$$\vec{f}_1 = \vec{f}(\vec{X})$$

$$\vec{f}_2 = \vec{f}\left(\vec{X} + \frac{1}{2} h \vec{f}_1\right)$$

$$\vec{f}_3 = \vec{f}\left(\vec{X} + \frac{1}{2} h \vec{f}_2\right)$$

$$\vec{f}_4 = \vec{f}(\vec{X} + h \vec{f}_3)$$

The next \vec{X} can be approximated by

$$\vec{X}_{next} = \vec{X} + \frac{h}{6} [\vec{f}_1 + 2(\vec{f}_2 + \vec{f}_3) + \vec{f}_4]$$

with an error of fifth power term of the Taylor series expansion. The h is the increment step side.

Recall,

$$m\ddot{x} = \frac{A\mu_o N^2 (g_o I_o + x i) (g_o i + I_o x)}{(g_o^2 - x^2)^2}$$

$$v = R i + L \frac{di}{dt}$$

Let

$$x_1 = x = \text{output}$$

$$x_2 = \frac{dx_1}{dt}$$

$$x_3 = i$$

$$x_4 = t$$

$$v = u = \text{input}$$

So

$$\dot{x}_1 = x_2$$

$$\dot{x}_2 = \ddot{x} = \frac{\frac{A \mu_o N^2}{m} (g_o I_o + x_1 x_3) (g_o x_3 + I_o x_1)}{(g_o^2 - x_1^2)^2}$$

$$\dot{x}_3 = -\frac{R}{L} x_3 + \frac{1}{L} u$$

$$\dot{x}_4 = 1$$

Let the control law be

$$u = r - (k_1 x_1 + k_2 x_2 + k_3 \dot{x}_2)$$

where r is the reference input.

In the computer code, we need to estimate the second derivative of x , which is achieved by

$$(x_{2 \text{ present}} - x_{2 \text{ previous}}) / \text{time interval}$$

For the linearized plant dynamics equations, slightly modification of the computer codes can do the job. The results of computer simulation are shown in figure 14 to 19. The computer program was written in Pascal language, and is shown in Appendix IV.

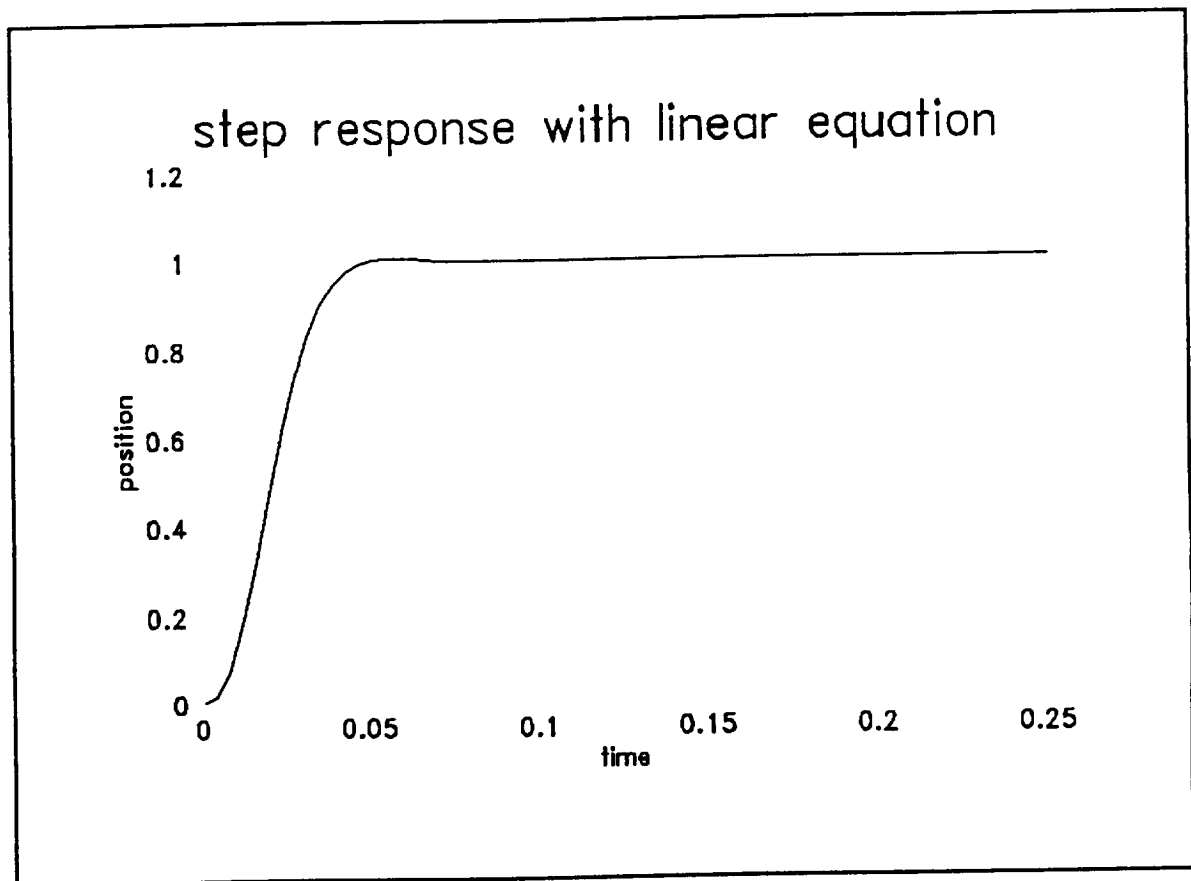


figure 14

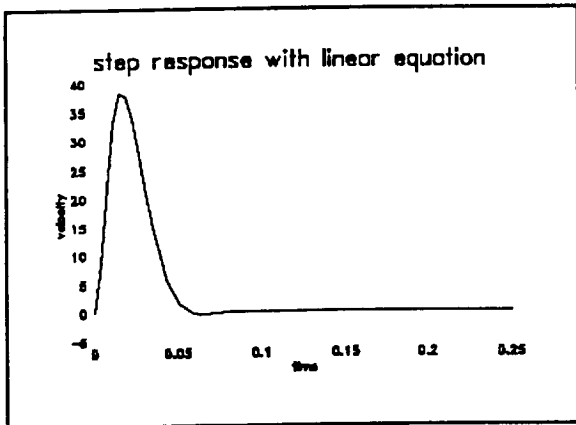


figure 15

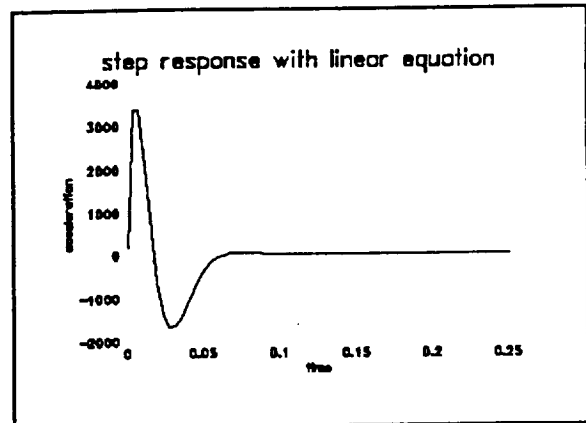


figure 16

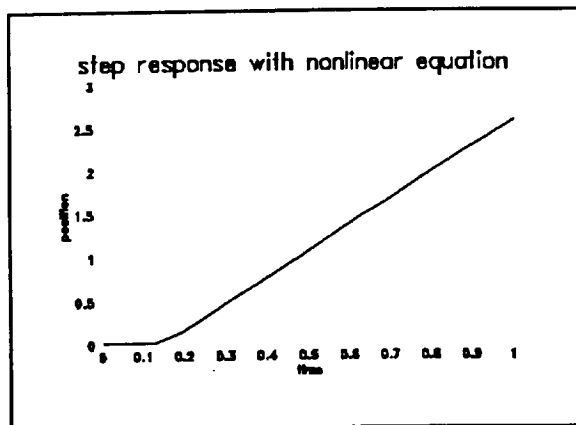


figure 17

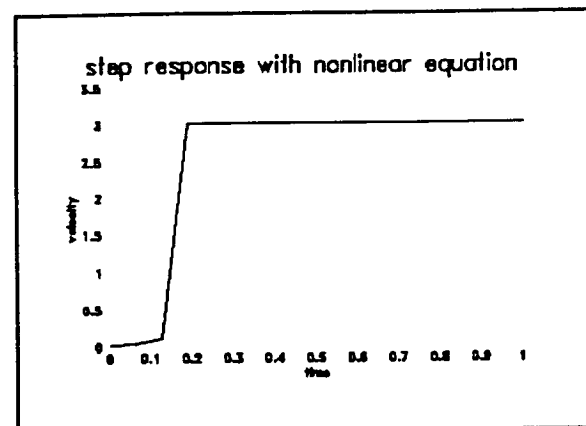


figure 18

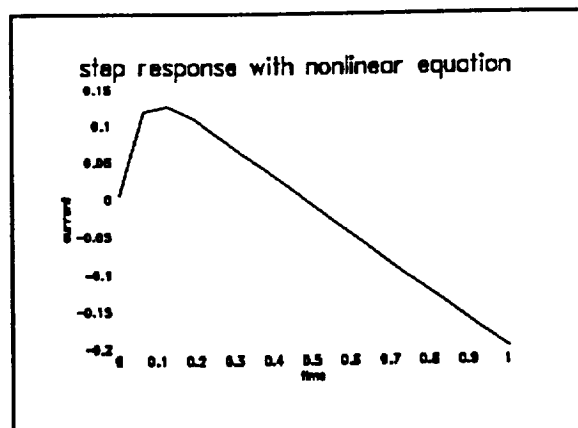


figure 19

V. Discussion of results

The computer simulation showed that the step response increased linearly with time, figure 17. That is, an unstable response occurred.

Consider the plant dynamics equations, recall

$$\dot{x} = \frac{A \mu_o N^2 (g_o I_o + x i) (g_o i + I_o x)}{(g_o^2 - x^2)^2}$$

$$\text{As for } |x| < |g_o|$$

$$\frac{1}{(g_o^2 - x^2)^2} = g_o^{-4} \frac{1}{(1 - \frac{x^2}{g_o^2})^2}$$

$$= g_o^{-4} [1 + (\frac{x^2}{g_o^2}) + (\frac{x^2}{g_o^2})^2 + \dots]^2$$

$$= g_o^{-4} [1 + 2(\frac{x^2}{g_o^2}) + 3(\frac{x^2}{g_o^2})^2 + \text{higher terms}]$$

$$\text{So } \frac{(g_o I_o + x i) (g_o i + I_o x)}{(g_o^2 - x^2)^2}$$

$$= g_o^{-4} (g_o I_o + x i) (g_o i + I_o x)$$

$$[1 + 2(\frac{x^2}{g_o^2}) + 3(\frac{x^2}{g_o^2})^2 + \text{higher terms}]$$

$$= g_o^{-4} (g_o I_o^2 x + g_o^2 I_o i + g_o x i^2 + I_o x^2 i)$$

$$[1 + 2(\frac{x^2}{g_o^2}) + 3(\frac{x^2}{g_o^2})^2 + \dots]$$

$$= g_o^{-4} [(g_o I_o^2 x + g_o^2 I_o i)$$

$$+ (2 \frac{I_o^2}{g_o} x^3 + 3 I_o x^2 i + g_o x i^2) + \text{higher terms}]$$

Obviously, the coefficient magnitude of the third terms in the Taylor's series expansion is larger than the coefficient magnitude

of the first term. Thus, at least, we need to include the third terms in the compensator design. However, we cannot use the conventional linear design theory in this situation.

Even though we include the third terms in the design, the coefficient magnitude of the x^n terms in the series expansion increase without bound (because $g_0 < 1$). So, the Taylor's series expansion does not exist.

VI. Conclusion and recommendation

The plant dynamics equations are nonlinear, and the conventional linearization does not work. We recommend to design the compensator without linearization in the time domain.

As, in general, if we close the loop,

$$\begin{aligned}\frac{d\vec{x}}{dt} &= \vec{f}(\vec{x}, u) \\ u &= g(r, \vec{x})\end{aligned}$$

define PI to be

$$\int_0^{\infty} t (x_1 - r)^2 dt$$

and, minimizing the PI which is subjected to the constraint equation,

$$\frac{d\vec{x}}{dt} = \vec{f}(\vec{x}, g(r, \vec{x}))$$

, by the Langrange multiple method. The mathematics is too difficult to carry out, and the analysis is left for interested reader only.

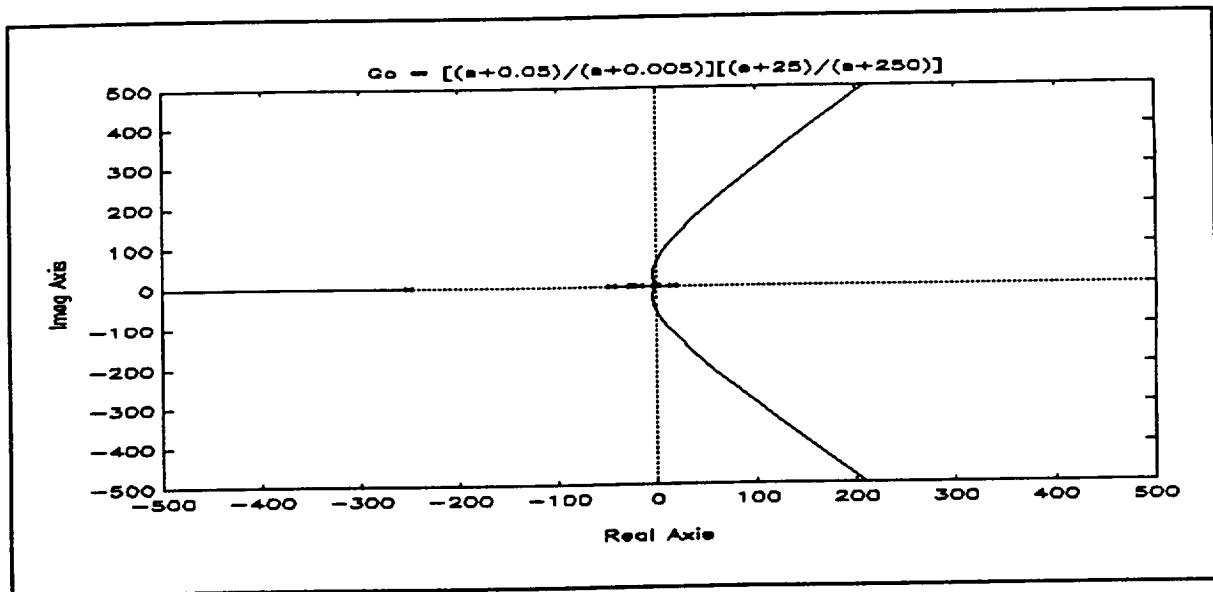
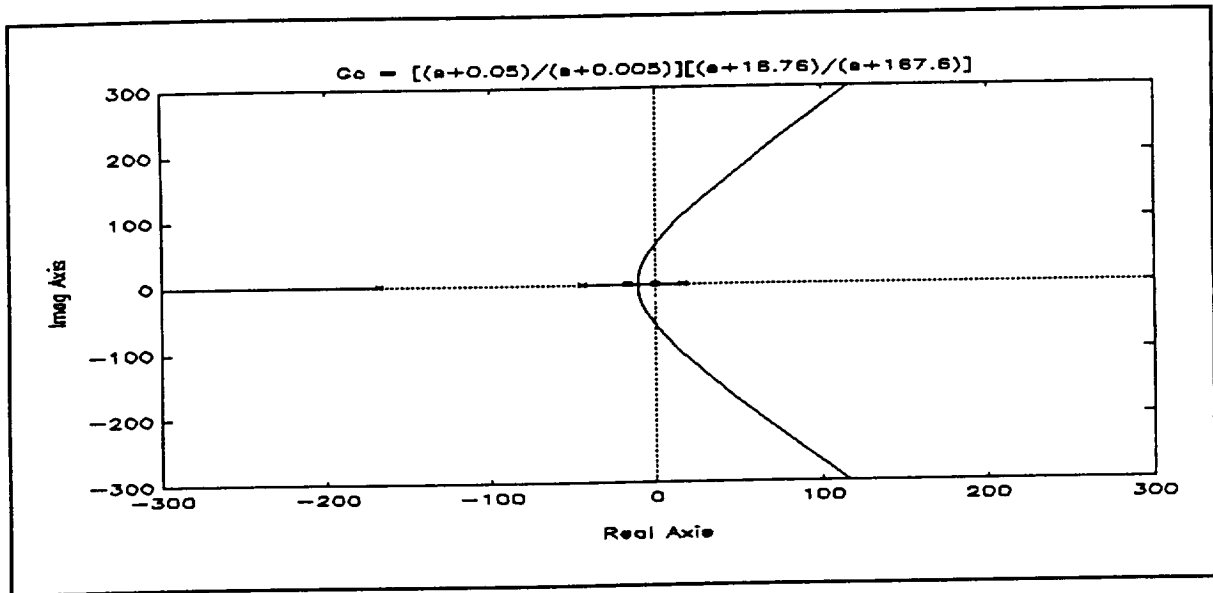
Bibliography

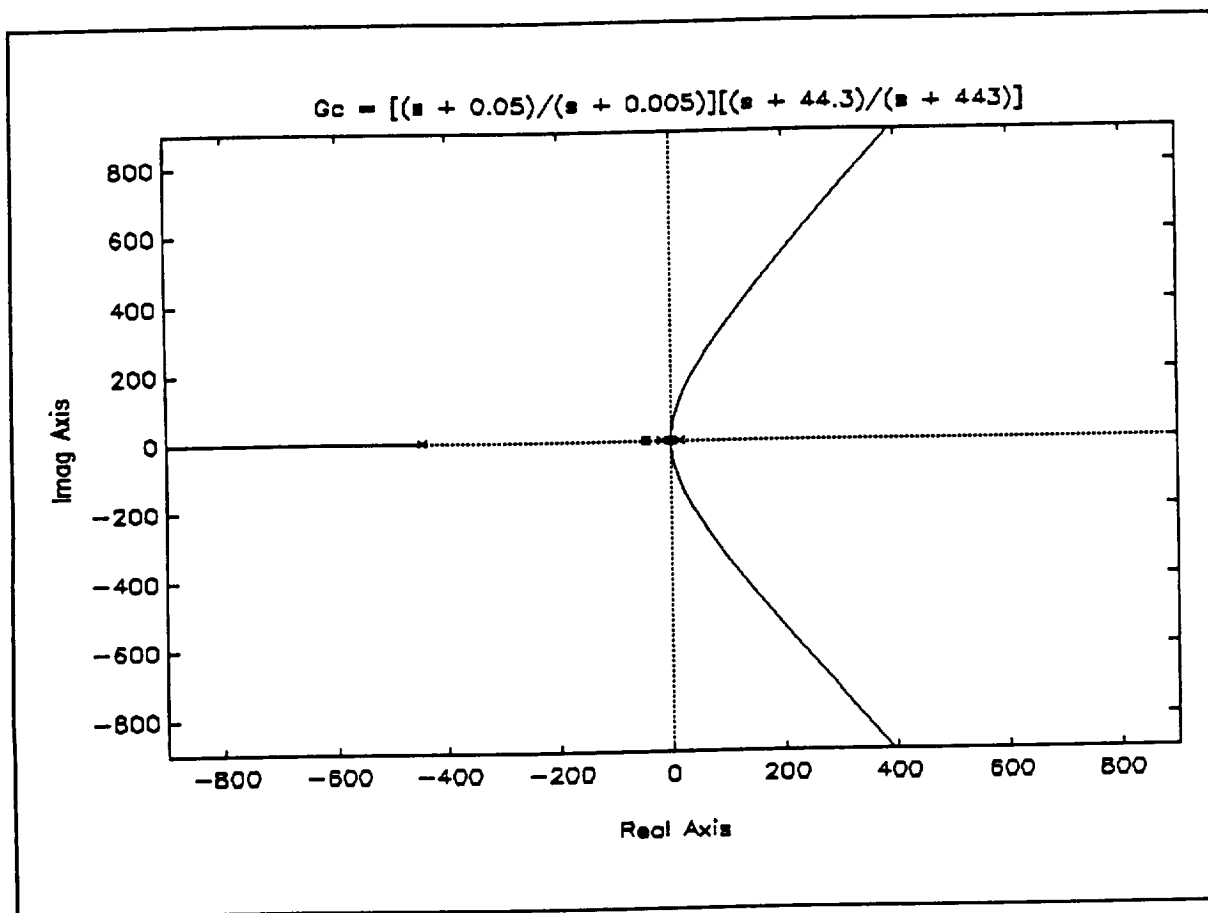
1. Jayawant, B.V. " Review Lecture of Electromagnetic Suspension and Levitation Techniques," Proc. R. Soc. Lond. A416, 245-320 (1988).
2. Groom, N.J. " ASPS Final Design Review," Sperry Corporation Flight Systems, May 1977.
3. Hamilton, B.J. " The Development of the ALPS Vernier System," NASA NAS1-15008, June 1983.
4. Woodson, H.H. and Melcher, J.R. *Electromechanical Dynamics. Part I: Discrete Systems.* John Wiley and Sons, Inc., 1968.
5. Bohr, E.V. *Introduction to Electromagnetic Fields and Waves.* Addison-Wesley Publishing Company, 1967.
6. Hayt, W.H. *Engineering Electromagnetic.* McGraw-Hill Book Company, 1981.
7. Humphris, R.R." Introduction to Magnetic Bearings," ROMAG 91, Magnetic Bearings and Dry Gas Conference and Exhibition, March, 1991.
8. Groom, N.J." Analytical Model of an Annular Momentum Control Device Laboratory Test Model Magnetic Bearing Actuator," NASA TM-80099, Aug., 1997.
9. Kilgore, W.A." Comparison of Digital Controllers used in Magnetic Suspension and Balance Systems," M.S. Thesis, Old Dominion University, Dec. 1989.

10. D'Azzo, J.J. *Linear Control Analysis and Design: Conventional and Modern*. McGraw-Hill Publishing Company, 3rd Ed., 1988.

Appendix I

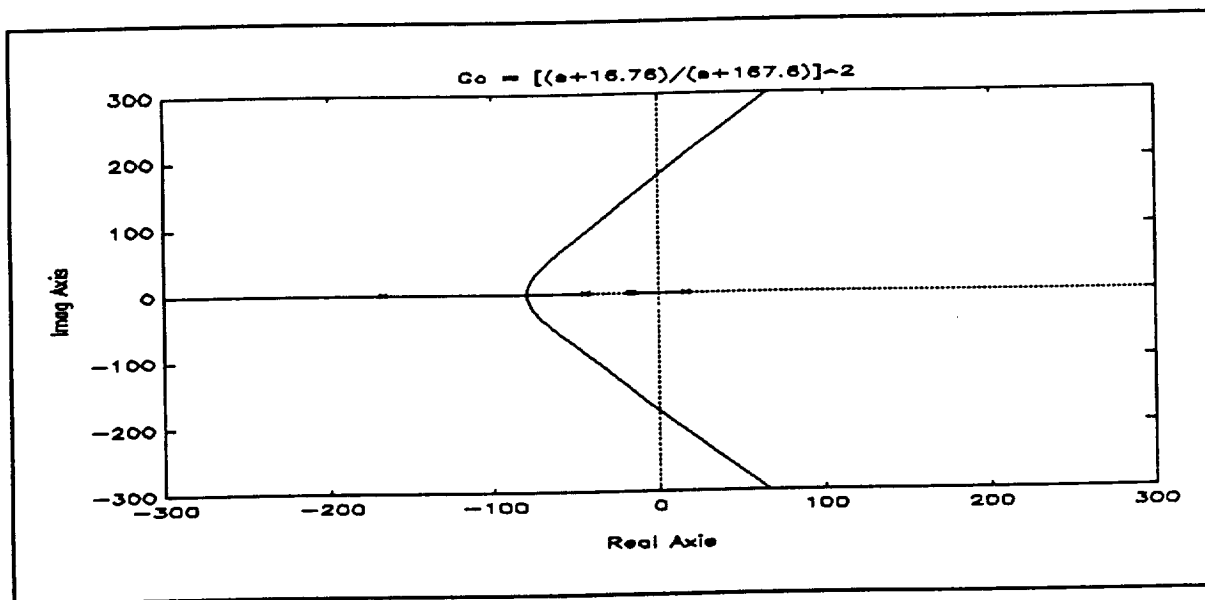
Root locus result of general lead lag cascade compensator



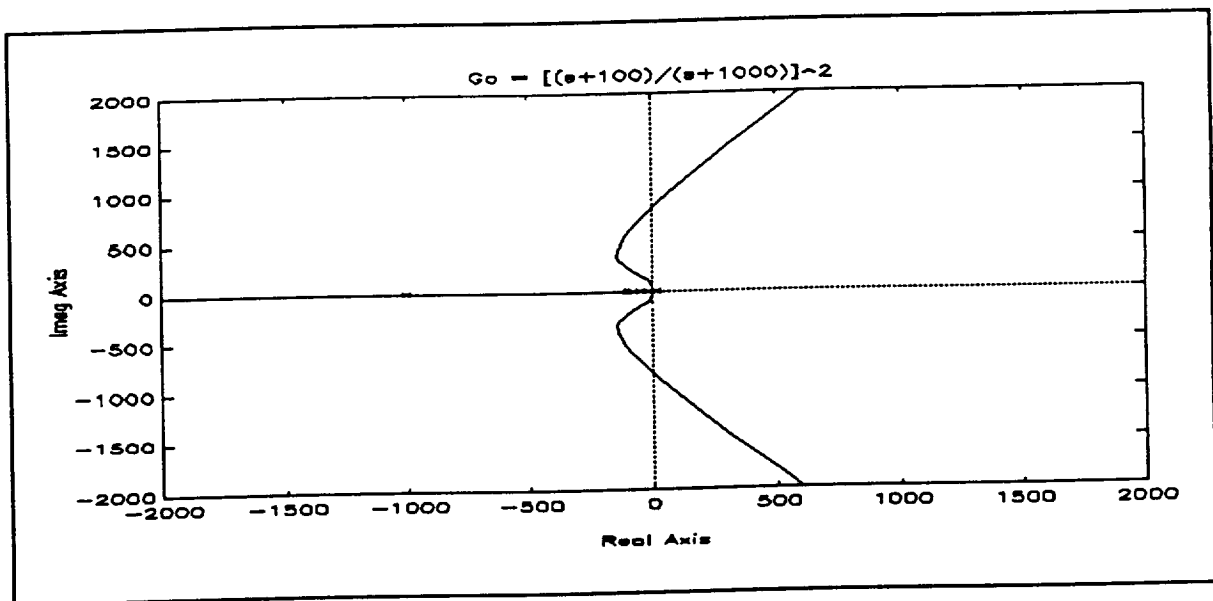
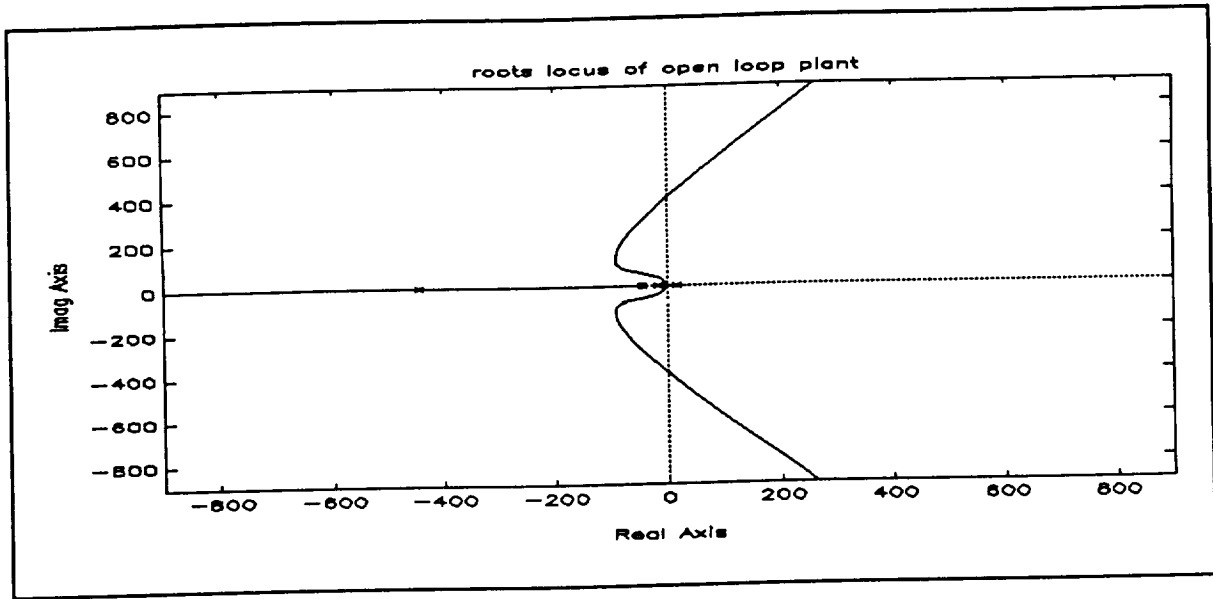


Appendix II

Root locus results of cascade dual phase advance compensator



$$G_c = [(s + 44.3)/(s + 443)]^2$$



Appendix III
state feedback design procedure¹⁰

Let the open-loop plant transfer function be

$$G_p = \frac{C_0}{s^3 + a_2 s^2 + a_1 s + a_0} = \frac{X}{u}$$

Let, for standard notation,

$$x_1 = y, \quad x_2 = \frac{dy}{dt}, \quad x_3 = \frac{d^2y}{dt^2}$$
$$\therefore \frac{dx_1}{dt} = \frac{dy}{dt} = x_2, \quad \frac{dx_2}{dt} = \frac{d^2y}{dt^2} = x_3, \quad \frac{dx_3}{dt} = \frac{d^3y}{dt^3}$$

and

$$\frac{dX}{dt} = A X + b u$$
$$y = [1 \ 0 \ 0] X = c^T X$$

Let the control law be

$$u = r - k^T X$$

where $k^T = [k_1 \ k_2 \ k_3]$

Consider

$$\begin{aligned}
 H(s) &= \frac{k^T X(s)}{Y(s)} = \frac{k^T X}{C^T X} \\
 &= \frac{k_1 x_1 + k_2 x_2 + k_3 x_3}{x_1} \\
 H(s) &= \frac{k_1 x_1 + k_2 s x_1 + k_3 s^2 x_1}{x_1} \\
 &= k_1 + s k_2 + s^2 k_3
 \end{aligned}$$

$$\therefore GH = \frac{c_0 (k_1 + s k_2 + s^2 k_3)}{s^3 + a_2 s^2 + a_1 s + a_0}$$

and the overall transfer function is

$$\begin{aligned}
 \frac{Y(s)}{R(s)} &= \frac{G}{1 + GH} = \frac{c_0}{(s^3 + a_2 s^2 + a_1 s + a_0) + c_0 (k_3 s^3 + k_2 s + k_1)} \\
 &= \frac{c_0}{s^3 + (a_2 + c_0 k_3) s^2 + (a_1 + c_0 k_2) s + (a_0 + c_0 k_1)}
 \end{aligned}$$

using the final value theorem,

$$\begin{aligned}
 \lim_{t \rightarrow \infty} y(t) &:= y_{ss} = \lim_{s \rightarrow 0} s Y(s) \\
 \therefore y_{ss}(t) &= \lim_{s \rightarrow 0} \frac{s c_0 R(s)}{s^3 + (a_2 + c_0 k_3) s^2 + (a_1 + c_0 k_2) s + (a_0 + c_0 k_1)}
 \end{aligned}$$

for step input $R(s) = s^{-1}$

$$\therefore y_{ss} = \frac{c_0}{a_0 + c_0 k_1} := 1 \text{ for zero error}$$

$$\text{ie, } k_1 = 1 - \frac{a_0}{c_0}$$

which is fixed. By appropriate selecting the value of k^T , we can implement any desired characteristic equation as we want.

observer design

original plant:

$$\frac{dX}{dt} = A X + b u$$

$$y = c^T X$$

Let \hat{x} be the estimated state vector.

Let

$$\frac{d\hat{x}}{dt} = A \hat{x} + b u + L (y - \hat{y})$$

$$\hat{y} = c^T \hat{x}$$

where L is the observer matrix

$$L = [l_1 \quad l_2 \quad l_3]$$

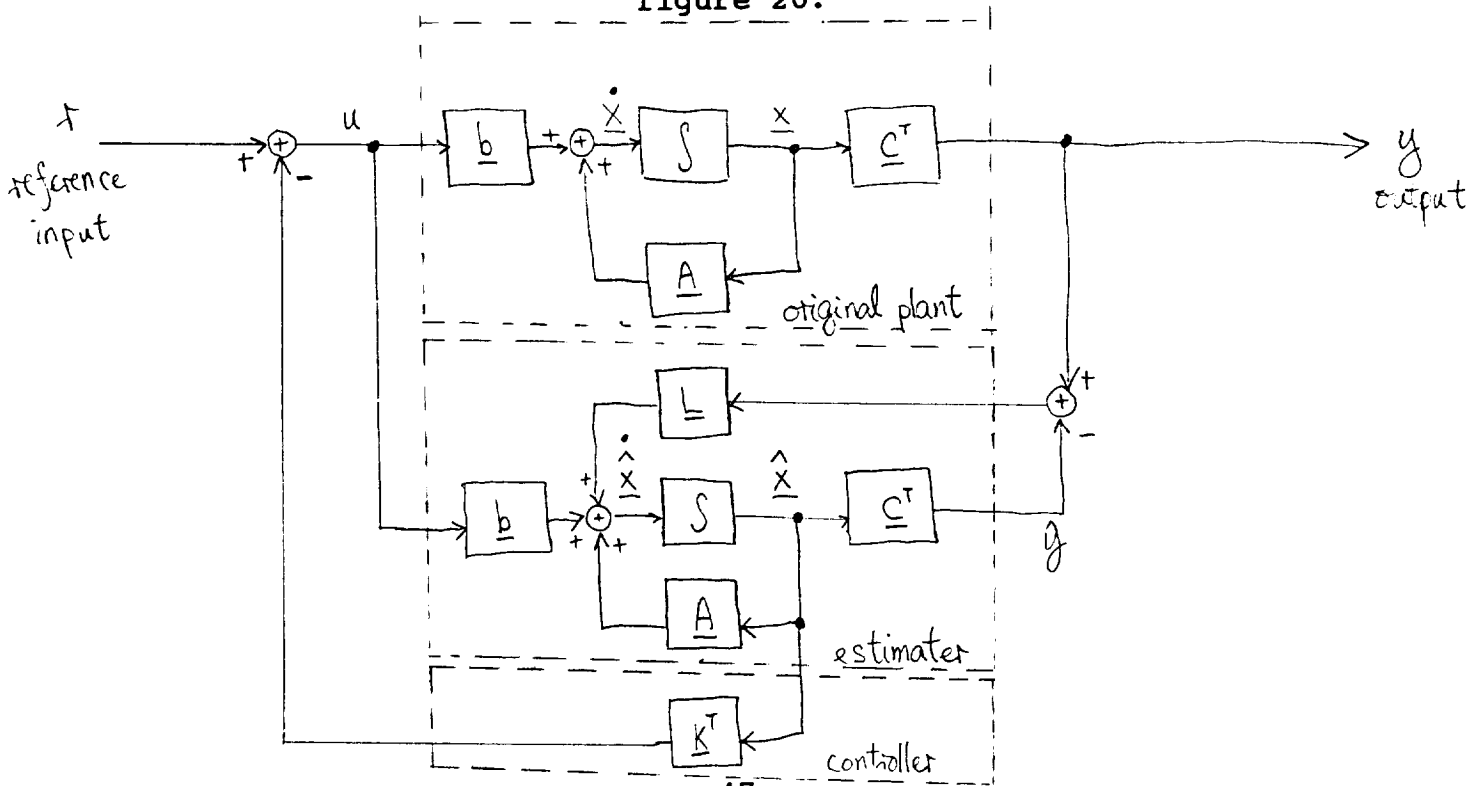
$$\text{define } e = x - \hat{x}$$

$$\rightarrow \frac{d e}{dt} = \frac{d x}{dt} - \frac{d \hat{x}}{dt}$$

$$\begin{aligned} &= A x + b u - (A \hat{x} + b u + L (c^T x - c^T \hat{x})) \\ &= A (x - \hat{x}) - L c^T (x - \hat{x}) \\ &= (A - L c^T) e \end{aligned}$$

By appropriate selecting the eigenvalues of e , the error of the estimated state vector will die out very quick. A state diagram is shown in figure 20.

figure 20.



Appendix IV

Computer codes for nonlinear plant dynamics

```
{ $N+, E+ }  
program project(outputo);           { 3\21\1993 }  
var  
  d:char;  
  i, j, n, nstep, e, b:integer;  
  h, h2, X1max, X4max, t, r, u, dum:real;  
  k:array[1..3] of real;  
  x,y:array[1..2,1..4] of real;  
  f:array[1..4,1..4] of real;  
  outputo:text;  
{ This is a Runge-Kntta method of order 4. }  
procedure initizing;  
begin  
  t:=0;           {initial time}  
  h:=1/1024;      {incremental time step}  
  n:=4;           {number of equations}  
  for i:=1 to 2 do {initial value}  
    for j:=1 to 4 do  
      begin  
        x[i,j]:=0;  
        y[i,j]:=0;  
      end;  
  for i:=1 to 4 do  
    for j:=1 to 4 do
```

```

        f[i,j]:=0;
nstep:=4096;          {number of step}

r:=1;

k[1]:=1.01;
k[2]:=0.021561;
k[3]:=0.0001505;

end;

procedure get_value_f;
begin
    f[e,1] := x[b,2];
    f[e,2] := (382.3996e-6)*(4.3434e-3 +
                        x[b,1]*x[b,3])*(0.00762*x[b,3] +
                        0.57*x[b,1])/(sqr(sqr(0.00762) - sqr(x[b,1])));
    dum := (y[b,2] - x[b,2])/h; {estimated the second derivate}
    u    := r - (k[1]*x[b,1] + k[2]*x[b,2] + k[3]*dum);
{control law}
    f[e,3] := -44.2995*x[b,3] + 5.5374*u;
    f[e,4] := 1;          { x[4]= time }
end;

procedure RK4SYS;
begin
    h2:=0.5*h;
    for j:=0 to nstep do
        begin

```

```

for e:=1 to 2 do
begin
    b:=e;
    get_value_f;
    for i:=1 to n do
        x[2,i]:=x[1,i] + h2*f[e,i];
    end;
    e:=3;
    get_value_f; {get f3}
    for i:=1 to n do
        x[2,i]:=x[1,i] +h*f[e,i];
    e:=4;
    get_value_f; {get f4}
    y[1,2]:=x[1,2];
    y[2,2]:=x[2,2];
    for i:=1 to n-1 do {compute next x(t+h)}

x[1,i]:=x[1,i]+h*(f[1,i]+2*(f[2,i]+f[3,i])+f[4,i])/6;
    x[1,4]:= t+j*h; {advance solution}
    if j mod 64 =0 then {write the result}
    begin
        for i:=1 to n do
            write(outputo,x[1,i],',');
            writeln(outputo);
            writeln(x[1,1],',',x[1,4]);
        end{if loop}

```

```

        end;{for j loop}
end;{RK4SYS}

begin {main}
    assign(outputo,'a:\p1.dat');
    rewrite(outputo);
    writeln(outputo);
    initizing;
    repeat
        RK4SYS;
        write('want change Y/N ?');
        readln(d);
        if d='y' then
            begin
                writeln('k1=',k[1],' k2=',k[2],' k3=',k[3]);
                write(' enter k1,k2,k3');
                readln(k[1],k[2],k[3]);
            end;
        until (d<>'y');
        writeln(outputo, ' Job completed. ');
        writeln(' Job completed. ');
        close(outputo);
end.

```